Boosting the Magnetic Field of a Torus-shaped Conductive Fluid via Poloidal Flow

Mamoru Otsuki[1*]

[1*]Independent, Tokyo, Japan.

Corresponding author(s). E-mail(s): gangankeisun@nifty.com;

Abstract

Researchers have struggled to understand the mechanism underlying the formation of celestial magnetic fields. Currently, the generation of axisymmetric and poloidal magnetic fields can be solved by complex convection arguments. There are also claims of simple convection, but these claims are not purely simple axisymmetric convection claims. This paper addresses a truly simple axisymmetric poloidal convection and magnetic field. To calculate the electrical components, this paper introduces a theory that separates the vector potential into inductance and current in a relational formula. The reason is to consider the mutual influence between distant circuits in terms of mutual inductance. That is, consider that each circuit is electrically affected by all other circuits. A solution that considers mutual influence can be obtained by using multiples of these equations as simultaneous equations and numerically calculating them as eigenvalue problems. The change in current is subsequently calculated from the change in inductance. Using this method, the generation of a simple axisymmetric poloidal magnetic field from axisymmetric poloidal convection is demonstrated. These concepts are novel, and we believe that these findings will contribute to further elucidating the formation mechanism of celestial magnetic fields. This work also disproves Cowling's theorem.

Keywords: poloidal flow, dynamo theory, inductance, numerically calculated eigenvalues, celestial magnetic field

1 Introduction

1.1 Magnetic Field Study of Celestial Bodies

Researchers have long struggled to understand the mechanism underlying the formation of celestial magnetic fields. Research in this field could progress through the discovery of a new underlying mechanism. Currently, the generation of axisymmetric and poloidal magnetic fields can be solved by complex convection arguments.

For example, the famous foundations for elucidating the mechanism of the formation of celestial magnetic fields are the ω effect[1], the α effect[2], and Cowling's theorem[3].

Taking the Sun as an example, the magnetic field in the plane perpendicular to the axis of rotation of the Sun is called the toroidal magnetic field, and the magnetic field in the plane parallel to the axis of rotation is called the poloidal magnetic field. The same is true for convection. According to Cowling's theorem, axisymmetric convection does not generate a stable axisymmetric magnetic field, either poloidal or toroidal.

The ω effect generates a toroidal magnetic field from a poloidal magnetic field where a gradient in angular velocity exists. Since the rotation of the surface of the Sun is faster at the equator than at the poles, an angular velocity gradient exists. If the initial magnetic field is poloidal, the magnetic field is stretched such that the angular velocity gradient winds it up, and the poloidal magnetic field becomes toroidal. If the toroidal magnetic field is changed to a poloidal magnetic field, the magnetic field may be amplified. However, no such effect was found. In the end, the result was in favour of Cowling's theorem.

The α effect assumes a velocity field that twists a magnetic field. The concept is to twist the toroidal magnetic field in some places and direct it in the poloidal direction. Therefore, if an α effect is added to the ω effect, mutual exchange of magnetic fields is possible, and the magnetic field may be amplified. However, this approach is not as easy to use as described above. Researchers have combined these effects with complex convection to further elucidate the mechanism of magnetic field generation[4][5]. To our knowledge, few papers[6][7][8] have argued for the generation of magnetic fields by simple convection. However, these claims are not purely simple axisymmetric convection claims.

The notion that a magnetic field is generated by complex convection or that an axisymmetric magnetic field does not occur constrains the study. A discussion of the generation of magnetic fields by complex convection is meaningful and necessary. However, in the observations, the difference between the axis of rotation and the magnetic axis is not large for the main celestial bodies in the solar system[1], especially for Saturn[9]. A theory that convection and magnetic fields are simply axisymmetric could facilitate a discussion.

Clarifying that simpler convection can generate a magnetic field will further advance research in this field. This paper[2] explores the possibility of generating a magnetic field by convection, which is simpler.

In this paper, we suggest the generation of a purely simple axisymmetric magnetic field via the following method.

[1]Note that this statement was made as a motivation for this study, and it is not known whether the results of this study are reflected in the nature of these celestial magnetic fields

[2]An earlier version of our original manuscript is available on a preprint server[10].

1.2 Methods for this Research

Before reading the following, it is necessary to understand the geometric structure of convection and inductance described in this paper. The convection and coil settings are described in detail in Section 2.1, Description of the Problem.

First, a formula is needed. We derive the basic electromagnetic induction equation to determine whether power generation starts and lasts. The relevant electromagnetic induction equations are expressed by the vector potential[11]. Furthermore, this vector potential is converted into an expression of inductance[11]. This conversion separates the vector potential into an inductance component representing the geometric structure of the fluid and an electrical component representing the current. With this equation, it is possible to calculate the electric current generated from changes in the geometric structure due to convection.

The reason is to consider the mutual influence between distant circuits in terms of mutual inductance. That is, consider that each circuit is electrically affected by all other circuits and cooperates to generate electricity. A solution that considers mutual influence can be obtained by using multiples of these equations as simultaneous equations and numerically calculating them as eigenvalue problems. The change in current is subsequently calculated from the change in inductance.

This electromagnetic induction equation is set and combined in a plurality of circuits. As a solution, the eigenvalues and eigenvectors are obtained. These results imply a change in the current and current distribution in the circuits. The results are shown in the tables and figures, showing the possibility of generating magnetic fields and the distribution of axisymmetric magnetic fields. Thus, it is shown that an axisymmetric magnetic field can be generated from axisymmetric convection without particularly complex convection.

1.3 The Role of the Formulas

A coil moving in a poloidal manner with convection moves in the radial direction and the cylindrical axial direction of the cylindrical coordinates. In this way, the coil moves in the existing magnetic field, and power generation occurs. The derived equation shows the relationship between this convection and power generation. The power generation also requires the generation of a stable magnetic field in the appropriate direction. This process is called self-excitation power generation. For this purpose, the equation is applied to a plurality of coils at different positions and solved as simultaneous equations. If power generation is recognised as a result of the calculation, the possibility of overall self-excited power generation of the torus can be explained.

1.4 Other Contents

Here, the possibility of growth of the magnetic field is shown, but the stability of the magnetic field is not indicated. We believe that a stable magnetic field is possible in relation to convection. However, since convection behaviour is not the subject of this paper, we discuss only the possibility of maintaining the stability of the magnetic field. This possibility is shown in Section 4.2, Possibility of Magnetic Field Stabilisation. The relationship with Cowling's theorem and others are discussed in Section 4, Discussion.

2 Mechanism

2.1 Description of the Problem

In this paper, we solve and discuss axisymmetric convection and magnetic fields via numerical calculations. Here, the geometric structure of convection and the knowledge necessary to calculate coil inductances are explained via figures.

To determine whether a magnetic field can fluctuate in the poloidal stream of a conductive fluid, a certain poloidal flow is set, and the electromagnetic induction equation is expressed in terms of toroidal vector potentials. The poloidal flow of a fluid occurs in a torus shape (Fig. 1). The upper figure is the whole, and the bottom figure is the cross section, where $\boldsymbol{U}$ is the poloidal velocity, R_0 is the radius of the poloidal flow, and r is the radius of an example position on the torus from the Z axis. The number of coils in the coil bundle is infinite. Here, only a part of the coils shown below are considered.

A representative cross section (Z-Y plane) of the torus is shown (Fig. 2(a)). The stream is divided into toroidal segments for calculation as coils (Fig. 2(b)). That is, Fig. 2(a) and (b) show the right half of the cross section of Fig. 1. Z is the centre axis, and Ra is the radial axis of the cylindrical coordinates (equivalent to the Y axis in Fig. 1), where the circle indicates the cross section of the torus. P_c is the centre of the flow, where r_0 and z_0 are the elements of position P_c in the Ra and Z directions, respectively. Notably, P_0 is at the coordinates (0,0), and P_c is at (r_0,0). P is a representative position at which the flow velocity vector $\boldsymbol{U}$ is calculated; u_r and u_z are the elements of $\boldsymbol{U}$ in the Ra and Z directions, respectively; θ is the angle between the position P and Ra axis; and r is the element of position P in the Ra direction (Fig. 2(a)). The coils used to define the flow torus are defined in Fig. 2(b). Sixteen coils are considered, where n indicates the number of the coil. The dotted lines indicate the coaxial coils (i.e., the region occupied by the fluid), which are separated by the thickness T. Multiple coils wind only once around the Z axis, and the coils move in the direction of $\boldsymbol{U}$ with radius R_0. Therefore, the circumference of each coil expands and contracts. The electric current runs separately in each coil in the ϕ direction, which orbits the Z axis. Although the coils can move, the later calculation of the eigenvalues assumes that they are motionless in a brief moment $\varDelta t$.

The top and side views of a set of any two coaxial coils are shown (Figs. 3(a) and (b)). These figures explain the relationship between the electric current $\boldsymbol{I}$ and vector potential[11] $\boldsymbol{A}$ for the calculation of inductances[11]. X, Y, and Z are the axes of the rectangular Cartesian coordinate system (Fig. 3). C_j is Coil j, in which the current $\boldsymbol{I}_j$ flows, and C_i is Coil i, which obtains the vector potential[11] $\boldsymbol{A}_j$ induced by the current $\boldsymbol{I}_j$ running in Coil C_j. ϕ is the angle of rotation around the Z axis, starting from the Y axis. Here, r_i and r_j are the radii of C_i and C_j, respectively. Furthermore, ds_i and ds_j are infinitesimal lengths of C_i and C_j , respectively, on each coil for integration, where ds_i is placed on C_i ($\phi = 0$) and where ds_j is placed on $\mathrm{P}_{j\phi}$ at ϕ with a distance l between them. $\boldsymbol{I}ds_j$ is the contribution to the current over ds_j, where $\boldsymbol{A}ds_j$ is the vector potential induced on ds_i by $\boldsymbol{I}ds_j$. $\boldsymbol{A}_j$ is the element of $\boldsymbol{A}ds_j$ in the X direction. $\varPhi_i$ is the total flux linked in C_i. The side view is also a schematic version of Fig. 2. The

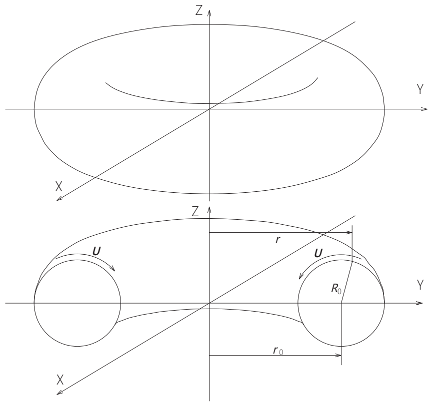

Fig. 1 Schematic of the toroidal geometry. This schematic is an approximate geometric outline of convection set by numerical calculations. A torus-like conductive fluid flows in a poloidal direction U. The upper figure is the whole, and the bottom figure is the cross section.

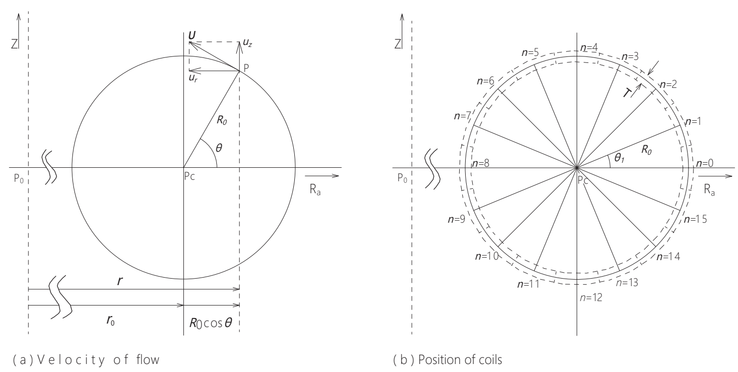

Fig. 2 Schematics of the (a) velocity of the fluid flow and (b) defined coils in the cross section of the convection (Z-Y or Z-Ra plane). This figure is a cross section of Fig. 1 and shows settings such as the arrangement of the virtual coils used in the numerical calculations.

symbols are the same as those in Fig. 2. The dashed circle approximately indicates the convection of the fluid. P_j and P_i are the positions of the two coils in the Z-Ra plane.

In addition, a 3D image of the coils is shown to clarify their relationships with each other (Fig. 4). Each coil is arrayed coaxially with the Z axis, and the coils are parallel to each other.

2.2 Calculation of the magnetic properties

In the numerical calculations in this paper, the electromagnetic induction equations are applied to multiple coils, and the current is calculated by combining these equations to solve them as an eigenvalue problem. Here, the underlying electromagnetic induction equation is derived. In addition, a method for calculating the inductance to be included in the numerical calculation is described.

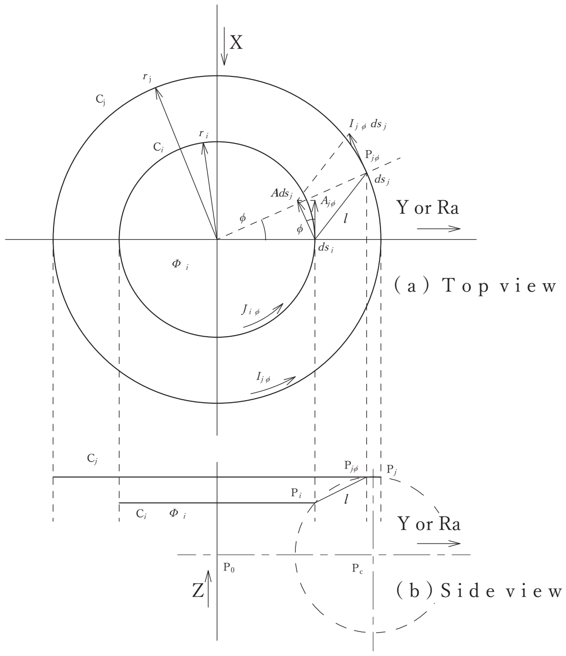

Fig. 3 Relationship between the electric current $\boldsymbol{I}$ and vector potential $\boldsymbol{A}$ for the set of coils shown in Fig. 2: (a) top view and (b) side view of the coils on the torus. Two virtual coils are used to explain how to calculate self- and mutual inductance.

2.2.1 Derivation of Basic Formulas

As a source equation for determining the relationship between the electric current and magnetic field, Ohm's law[11] is used with an electric field to calculate the current as follows:

$$\boldsymbol{J} = \sigma\left(\boldsymbol{E} + \boldsymbol{u} \times \boldsymbol{B}\right) \tag{1}$$

Here, $\boldsymbol{J}$ is the current density; σ is the electrical conductivity; $\boldsymbol{u}$ is the velocity of the conductive fluid; $\boldsymbol{B}$ is the magnetic field, which can be found via (2); $\boldsymbol{u} \times \boldsymbol{B}$ is the motion of the electric field; and $\boldsymbol{E}$ is the electric field potential, which can be found via (3)[11] as follows:

$$\boldsymbol{B} = \nabla \times \boldsymbol{A} \tag{2}$$

$$\boldsymbol{E} = -\frac{\partial \boldsymbol{A}}{\partial t} - \nabla \varphi \tag{3}$$

Here, φ is a scalar potential, $\boldsymbol{A}$ is a vector potential[11], and t represents the time.

To derive an induction equation expressed in vector potentials from Ohm's law, these equations are combined as follows:

$$\frac{\partial \boldsymbol{A}}{\partial t} - \boldsymbol{u} \times (\nabla \times \boldsymbol{A}) = -\nabla \varphi - \frac{\boldsymbol{J}}{\sigma} \tag{4}$$

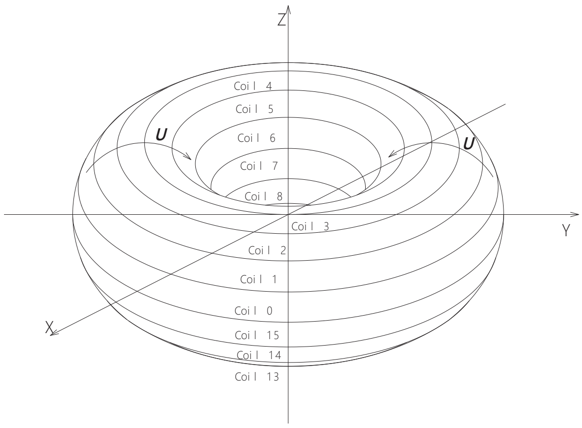

Fig. 4 3D view of the coaxial coils. A bird's-eye view is used to facilitate imagining the arrangement of the virtual coil.

To apply this induction equation for coils, the factor $2\pi r_i$ (r_i=coil C_i radius) is multiplied as an integral around the coil on both sides of the equation because $\boldsymbol{A}$ and the current density are the same around C_i.

$$\frac{\partial}{\partial t}(2\pi r_i \boldsymbol{A}) - \boldsymbol{u} \times (\nabla \times 2\pi r_i \boldsymbol{A}) = -\frac{2\pi r_i}{\sigma}\boldsymbol{J} \tag{5}$$

Here, φ is ignored because it is assumed that going around along C_i at that gradient will result in a value of zero. In this paper, the left-side second term of (5) is referred to as the induction term, and right-side of (5) is referred to as the attenuation term. Furthermore, (6) shows the relationship between $\boldsymbol{A}$ and the inductance[11] (L). Here, the total magnetic flux linking the coil, $\varPhi$, is used in place of L, where $\varPhi = LI$. The subscripts i and j refer to the coil numbers defined in Fig. 2, enabling the development of simultaneous equations.

$$\varPhi_i = \oint_{C_i} \boldsymbol{A}_j ds_i \tag{6}$$

Here, $\varPhi_i$ is the flux of coil C_i, and ds_i is an infinitesimal part of coil C_i. In this arrangement of coils, all the coils are arrayed coaxially with the Z axis and parallel to each other. Thus, $\boldsymbol{A}_j$ is the same around C_i. Therefore, $\varPhi_i = 2\pi r_i \boldsymbol{A}_j$. When $\varPhi_i = L_{ij} I_j$, the relationship between L_{ij} and $\boldsymbol{A}_j$ is as follows. L_{ij} is a matrix representing inductance, but only the diagonal element is self-inductance, and the other elements are mutual inductances, so it is hereafter referred to as M_{ij}.

$$\boldsymbol{A}_j = \frac{\boldsymbol{I}_j}{2\pi r_i} M_{ij}, A_{j\phi} = \frac{I_{j\phi}}{2\pi r_i} M_{ij} \tag{7}$$

$\boldsymbol{A}_j$ and $\boldsymbol{I}_j$ have only a toroidal component (indicated by the subscript ϕ) along the coil. Using (7), the vector potential is separated into an inductance component that expresses the structure of the fluid (electric circuits) and an electrical component that expresses the current. The reason is to consider the mutual influence between distant circuits in terms of mutual inductance. The change in current is subsequently calculated from the change in inductance. By substituting (7) into (5), the following equation is obtained:

$$\frac{\partial}{\partial t}\left(M_{ij}I_{j\phi}\right)-\left[\boldsymbol{u}\times\left(\nabla\times 2\pi r_i\boldsymbol{A}_j\right)\right]_\phi=-\frac{2\pi r_i}{\sigma}\boldsymbol{J}_i=-\frac{2\pi r_i}{\sigma}J_{i\phi} \tag{8}$$

Here, σ is the conductance of the fluid, and r_i is the radius from the Z axis. The current density $\boldsymbol{J}_i$ of the attenuation term is also described as $J_{i\phi}$ since it has only a ϕ direction component. However, the second term on the left-hand side of (8) is complicated. Thus, it must be addressed separately. This term is considered by decomposing it as follows:

$$\begin{aligned}\boldsymbol{u}\times\left(\nabla\times\boldsymbol{A}_j\right)&=\begin{bmatrix}u_{ir}\\0\\u_{iz}\end{bmatrix}\times\begin{bmatrix}\frac{1}{r_i}\left(-r_i\frac{\partial A_{j\phi}}{\partial z_i}\right)\\0\\\frac{1}{r_i}\left(\frac{\partial r_iA_{j\phi}}{\partial r_i}\right)\end{bmatrix}\\&=\begin{bmatrix}u_{ir}\\0\\u_{iz}\end{bmatrix}\times\begin{bmatrix}-\frac{\partial A_{j\phi}}{\partial z_i}\\0\\\frac{1}{r_i}A_{j\phi}+\frac{\partial A_{j\phi}}{\partial r_i}\end{bmatrix}\\&=\begin{bmatrix}0\\-u_{iz}\frac{\partial A_{j\phi}}{\partial z_i}-u_{ir}\left(\frac{1}{r_i}A_{j\phi}+\frac{\partial A_{j\phi}}{\partial r_i}\right)\\0\end{bmatrix}\end{aligned} \tag{9}$$

Here, rot$\boldsymbol{A}_j$ is decomposed into cylindrical coordinates, and the subscripts r, ϕ, and z indicate the component directions in cylindrical coordinates, namely, the radius from the Z axis, the angle around the Z axis, and the Z direction, respectively. Since the current only runs through the toroidal coil, only the toroidal $A_{j\phi}$ component remains with the vector potential. Furthermore, since it is uniform in the toroidal direction, the $\frac{\partial}{\partial\phi}$ component is zero, and the description is excluded. Therefore, $\boldsymbol{A}_j$ only has a component in the ϕ direction. Thus, the other components of $\boldsymbol{A}_j$ are omitted. (10) is obtained by multiplying (9) by $2\pi r_i$, substituting (7) and including only the ϕ component as follows:

$$\begin{aligned}&2\pi r_i\left[-u_{iz}\frac{\partial A_{j\phi}}{\partial z_i}-u_{ir}\left(\frac{1}{r_i}A_{j\phi}+\frac{\partial A_{j\phi}}{\partial r_i}\right)\right]\\&=-u_{iz}\frac{\partial M_{ij}I_{j\phi}}{\partial z_i}-u_{ir}\left(\frac{1}{r_i}M_{ij}I_{j\phi}+\frac{\partial M_{ij}I_{j\phi}}{\partial r_i}\right)\\&=-u_{ir}\frac{\partial M_{ij}I_{j\phi}}{\partial r_i}-u_{iz}\frac{\partial M_{ij}I_{j\phi}}{\partial z_i}-u_{ir}\frac{1}{r_i}M_{ij}I_{j\phi}\end{aligned} \tag{10}$$

(10) indicates the electromotive force. The electromotive force is unaffected by the cross-sectional area of the electric circuit. These terms are replaced by the second term on the left-hand side of (8) to obtain (11) as follows:

$$\frac{\partial}{\partial t}\left(M_{ij}I_{j\phi}\right)-\left(-u_{ir}\frac{\partial M_{ij}I_{j\phi}}{\partial r_i}-u_{iz}\frac{\partial M_{ij}I_{j\phi}}{\partial z_i}-u_{ir}\frac{1}{r_i}M_{ij}I_{j\phi}\right)$$

$$= -\frac{2\pi r_i}{\sigma} J_{i\phi}. \tag{11}$$

The left-side of (11) is expressed by the current $I_{j\phi}$, which is unaffected by the cross-sectional area, S, of the electric circuit. The attenuation term in (11), including the current density $J_{i\phi}$ is affected by the cross-sectional area of the circuit. The current density $J_{i\phi}$ of the attenuation term is $\frac{I_{i\phi}}{S}$. It is arranged as follows:

$$\begin{aligned}\frac{\partial}{\partial t}\left(M_{ij} I_{j\phi}\right) + u_{ir}\frac{\partial M_{ij} I_{j\phi}}{\partial r_i} + u_{iz}\frac{\partial M_{ij} I_{j\phi}}{\partial z_i} + u_{ir}\frac{1}{r_i} M_{ij} I_{i\phi} \\ = -\frac{2\pi r_i}{\sigma S} I_{i\phi}\end{aligned} \tag{12}$$

Since the first three terms on the left-hand side of (12) are equivalent to a total differential, they can be replaced as follows:

$$\frac{d}{dt}\left(M_{ij} I_{j\phi}\right) + u_{ir}\frac{1}{r_i} M_{ij} I_{j\phi} = -\frac{2\pi r_i}{\sigma S} I_{i\phi}$$

This equation can be transformed and rearranged as follows:

$$\frac{dM_{ij}}{dt} I_{j\phi} + M_{ij}\frac{dI_{j\phi}}{dt} + u_{ir}\frac{1}{r_i} M_{ij} I_{j\phi} = -\frac{2\pi r_i}{\sigma S} I_{i\phi}$$

$$\frac{dI_{j\phi}}{dt} = M_{ij}^{-1}\left(-\frac{dM_{ij}}{dt} I_{j\phi} - u_{ir}\frac{1}{r_i} M_{ij} I_{j\phi} - \frac{2\pi r_i}{\sigma S} I_{i\phi}\right)$$

As such, $I_{j\phi}$ cannot be obtained because the equation is a mixture of $I_{j\phi}$ and $I_{i\phi}$. The resistance matrix R_{ij} is adopted to unify to $I_{j\phi}$. The details are shown below.

$$\Lambda I_{j\phi} = -M_{ij}^{-1}\frac{dM_{ij}}{dt} I_{j\phi} - M_{ij}^{-1} u_{ir}\frac{1}{r_i} M_{ij} I_{j\phi} - M_{ij}^{-1} R_{ij} I_{j\phi} \tag{13}$$

(13) is obtained. Here, Λ indicates the eigenvalues. In this paper, we use this simultaneous equation to find the Λ value.

$\frac{2\pi r_i}{\sigma S}$ is the resistance sequence R_i. R_i is a function of the coil circumference and cross-sectional area S, where S is calculated from the thickness T and the section of the flow course as $S = \left(2\pi R_0 T\right)/16$. Then, $R_i = 2\pi r_i / \left(\sigma S\right) = \left(16 r_i\right) / \left(\sigma R_0 T\right)$. The resistance matrix R_{ij} is constructed from R_i such that $R_i I_{i\phi} = R_{ij} I_{j\phi}$. Specifically, R_{ij} is a diagonal matrix in which R_i is arranged diagonally.

The matrix summarizing the right-hand side of (13) is a real symmetric matrix[3], and the eigenvalues are real numbers. Since it does not contain imaginary numbers, it would not imply precession or oscillation.

2.2.2 Method for Calculating the Inductance

The inductance used in the example calculation (see Figs. 3(a) and (b)) is as follows. In the coil description (Fig. 2), the coil's cross-sectional area and shape are disregarded to calculate the inductance because these geometrical factors introduce a large degree of complexity. Therefore, the coil is treated in the calculation, and Fig. 3 is approximated as a thin line. $\boldsymbol{A}_j$ is calculated[12] as follows:

[3] not exactly. See Section 4.5, Alternating Matrix Components.

$$\boldsymbol{A}_j = \frac{\mu}{4\pi}\oint_{C_j}\frac{\boldsymbol{J}_j}{l}dV = \frac{\mu}{4\pi}\oint_{C_j}\frac{\boldsymbol{J}_j S}{l}ds_j = \frac{\mu}{4\pi}\oint_{C_j}\frac{\boldsymbol{I}_j}{l}\cos\phi ds_j$$
$$= \frac{\mu}{4\pi}\boldsymbol{I}_j\oint_{C_j}\frac{\cos\phi}{l}ds_j, \tag{14}$$

where l is the distance between ds_i and ds_j, μ is the magnetic permeability, dV is the infinitesimal volume, and S is the cross-sectional area of the current (i.e., the coil). When only ϕ directional components are handled, $I_{j\phi} = J_{j\phi}S$ is the current, and the directional element for ds_i of $I_{j\phi}$ is $I_{j\phi}cos\phi$. By substituting (7) for $A_{j\phi}$ in (14), (15) is obtained as follows:

$$M_{ij} = \frac{2\pi r_i}{I_{j\phi}}\frac{\mu}{4\pi}I_{j\phi}\oint_{C_j}\frac{\cos\phi}{l}ds_j = 2\pi r_i\frac{\mu}{4\pi}\oint_{C_j}\frac{\cos\phi}{l}ds_j \tag{15}$$

When μ is set to $4\pi\times10^{-7}$H/m (vacuum conditions), (16) is obtained as follows:

$$M_{ij} = 2\pi r_i\oint_{C_j}\frac{\cos\phi}{l}ds_j\times10^{-7} \tag{16}$$

M_{ij} is calculated by summing (17), where C_j is divided into $k = 100$ equal parts, $\Delta s_j = \frac{2\pi r_j}{100}$, as follows:

$$M_{ij} \approx 2\pi r_i\sum_{k=1}^{100}\frac{\cos\phi_k\Delta s_j}{l_k}\times10^{-7} \tag{17}$$

$$l_k = \sqrt{(r_j\cos\phi_k - r_i)^2 + (r_j\sin\phi_k)^2 + (z_j - z_i)^2} \tag{18}$$

The angle of a specific coil n is given by $\theta_n = 2\pi n/16$, where $r_n = r_0 + R_0\cos\theta_n$ and $z_n = R_0\sin\theta_n$ (Fig. 2). Previously, i and j were used in mutual inductance calculations to distinguish between the coils that received electromotive force and the coils that had a current flow. Each number n is replaced by i or j for any two of the coils.

2.2.3 Elements of other Expressions

$\frac{dM_{ij}}{dt}$ is calculated as the difference in M_{ij} induced by the flow velocity over an infinitesimal divided by $\Delta t(ex.1.0\times10^{-6}s)$.

The velocity $\boldsymbol{U}$ depends on the θ_n of each coil and is calculated as follows (Fig. 2):

$$|\boldsymbol{U}| = \frac{r_0}{r_i}\omega R_0,\ u_r = -|\boldsymbol{U}|\sin\theta_n,\ u_z = |\boldsymbol{U}|\cos\theta_n. \tag{19}$$

where ω is the angular velocity of the flow. $\frac{1}{r_i}$ is multiplied because a fluid of the same volume is concentrated and dispersed towards the Z axis in a poloidal flow such that the flow path expands and contracts, and the velocity changes accordingly. $\frac{r_0}{r_i}$ is a coefficient that adjusts on the basis of the position of r_0 so that the flow rate satisfies the continuity equation.

Furthermore, M_{ij}^{-1} is the inverse matrix of M_{ij}.

Table 1 Eigenvalues Λ. The eigenvalue is calculated numerically. Assuming the boundary of the start of magnetic field generation, the calculation condition was set to generate one eigenvalue that was barely positive. Therefore, only λ_{16} is positive.

Λ	Eigenvalue	Λ	Eigenvalue
λ_1	-5.290×10^{-1}	λ_9	-8.964×10^{-2}
λ_2	-3.221×10^{-1}	λ_{10}	-6.714×10^{-2}
λ_3	-2.288×10^{-1}	λ_{11}	-6.575×10^{-2}
λ_4	-1.762×10^{-1}	λ_{12}	-5.037×10^{-2}
λ_5	-1.431×10^{-1}	λ_{13}	-4.163×10^{-2}
λ_6	-1.208×10^{-1}	λ_{14}	-2.918×10^{-2}
λ_7	-1.084×10^{-1}	λ_{15}	-1.633×10^{-2}
λ_8	-9.134×10^{-2}	λ_{16}	$\mathbf{7.729 \times 10^{-3}}$

Table 2 Eigenvector of the maximum eigenvalue in Table 1. This eigenvector corresponds to the current distribution flowing through each coil. The combined current is adjusted to 1. The current is maximised at Coil 6.

Coil number	Eigenvector	Coil number	Eigenvector
0	2.262×10^{-2}	8	1.193×10^{-1}
1	4.870×10^{-2}	9	-5.597×10^{-2}
2	9.259×10^{-2}	10	-6.638×10^{-2}
3	1.691×10^{-1}	11	-4.792×10^{-2}
4	2.979×10^{-1}	12	-3.188×10^{-2}
5	4.806×10^{-1}	13	-1.899×10^{-2}
6	$\mathbf{6.198 \times 10^{-1}}$	14	-7.231×10^{-3}
7	4.801×10^{-1}	15	5.626×10^{-3}

3 Calculation Conditions and Results

3.1 Calculation conditions

The conditions for the numerical calculations are as follows.

The general conditions are $R_0 = 1000$ m, $r_0 = 2000$ m, and $T = 0.1R_0$. The electrical conductivity σ is 10^3 s/m (solar convection zone)[9]. The velocity of convection is given by (19), where $|\boldsymbol{U}| = \frac{r_0}{r_i}\omega R_0$. As a condition, the angular velocity ω is set to $2\pi 2.1 \times 10^{-3}$, where only the maximum eigenvalue is barely positive. In other words, we set the conditions that seem to be the boundary at which power generation begins to occur.

3.2 Results

The result calculated on the basis of (13) is shown under the conditions above. The eigenvalues $\Lambda(\lambda_1 - \lambda_{16})$ are listed in Table 1. A positive value is highlighted in bold in the table. Only the maximum eigenvalue, λ_{16}, has positive polarity. Although it has positive polarity, the absolute value is small. This result is obtained because the

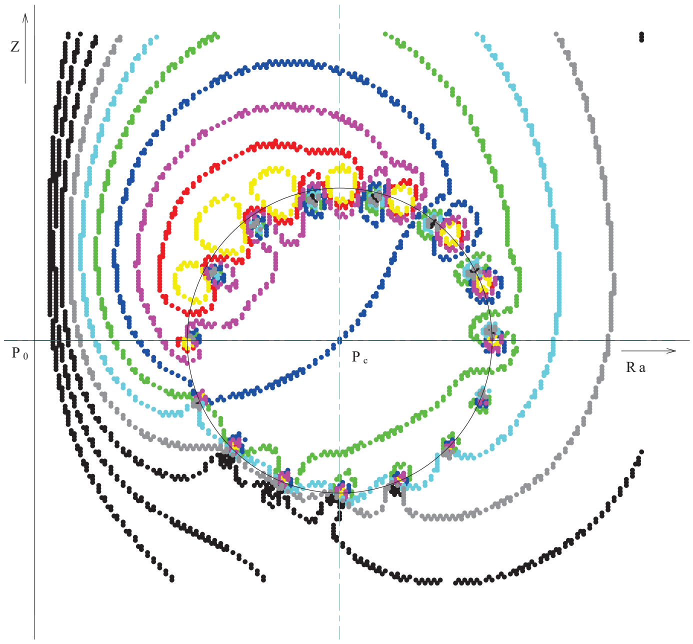

Fig. 5 Magnetic force contour lines generated from the current state on the basis of the results of the numerical calculations. This figure shows the magnetic force contour lines drawn on the Z-Ra plane on the basis of eigenvectors (Table 2). The range of the figure is $\pm 2R_0$ in the Z direction and $+4R_0$ in the Ra direction. Since the magnetic field is not a specific value that has increased, its unit is not displayed. Ten contour lines are displayed. A strong magnetic field is displayed in a warm colour.

calculation conditions were set in a specific way. Thus, under these conditions, power generation begins. In addition, if the convection speed is high, the power generation will be strong. The eigenvector of the maximum eigenvalue is shown in Table 2. The length of each component of this eigenvector is adjusted so that the norm is 1. These components indicate the current values of each coil. This condition indicates that the absolute value of the current is maximised in Coil 6, which is highlighted in bold. This table is used to create the following figure.

The calculation method of the magnetic field is as follows. The calculation of the inductance is obtained through the calculation of the vector potential, as shown in (14). Therefore, the vector potential was calculated using the inductance calculation method. That is, via (7), the vector potential was obtained through the current of the coil and the temporary inductance at each location. Furthermore, the value related to the rotation of the vector potential at each location was obtained and converted to a magnetic field via (2). In Fig. 5, the intensity of the magnetic force is represented by contour lines. On a poloidal surface, it is a line, but in three-dimensional space, it is a curved surface whose line is rotated on the axis of symmetry. Since it is a cylindrical coordinate, the magnetic force, that is, the magnetic flux density, even if the same number of magnetic fluxes passes, the cross-sectional area of the passage changes according to the distance r from the axis of rotational symmetry Z, so the

Table 3 Maximum eigenvalue and maximum eigenvalue without the second term on the right-hand side of (13) at the angular velocity of convection at which power generation starts.

R_0 km	ω rad/s	λ_{max}	$\lambda_{max}N$
1	$2\pi 2.1 \times 10^{-03}$	7.729×10^{-03}	3.578×10^{-04}

magnetic flux density changes. Therefore, in the contour line, the magnetic force is corrected by multiplying the circumference by $2\pi r$.

In Fig. 5, the yellow pointillism line is the highest magnetic field level (warmer colours have a higher level). The circle in the figure is the hypothetical convection position shown in Fig. 2. Since there are yellow areas around the second quadrant (top left of P_c) of this circle, it is thought that power generation mainly occurs there. In this study, convection is examined only at the position of 16 coils on the convective circle shown in Fig. 2, so it is difficult to understand because the contour lines of the same level are divided into multiple parts and are intricate near the convection. In reality, the coils should be innumerably distributed so that the contour lines are continuous and smooth.

Fig. 5 shows that the coils are rotationally symmetric around the Z-axis, and numerical calculations show that an axisymmetric magnetic field arises from axisymmetric poloidal convection on the same axis.

3.3 Potential Power Generation Capacity

Furthermore, the second term on the right-hand side of (13) plays an important role. According to the estimation, the eigenvalue λ_{max} when this term is included, as shown in Table 3, is more than one order of magnitude larger than λ_{max}N when it is omitted. This result is obtained because once power generation starts, the term works more strongly because of the generated current, and power generation becomes more powerful.

4 Discussion

As described above, the underlying electromagnetic induction equation was derived, and the result was obtained via numerical calculation. The results revealed the start of power generation by generating an axisymmetric magnetic field from poloidal convection. Here, the evaluation and problems of this numerical calculation are discussed in detail below.

4.1 Generation of Axisymmetric Magnetic Fields

The following discussion can be drawn from Fig. 5.

A strong magnetic field originates around the second quadrant of convection and passes through the convection circle. In other words, a strong magnetic field intersects with convection and seems to contribute to power generation. In addition, outside the strong magnetic field, a weak magnetic field passes near the Z-axis and circulates on the outside away from convection. Since this surface is rotationally symmetric around the Z axis, it shows a rotationally symmetrical magnetic force in the poloidal flow.

4.2 Possibility of Magnetic Field Stabilisation

When the current increases to a certain extent, the Lorentz force acts. This force acts in the opposite direction of convection, thus reducing the flow velocity. This behaviour will suppress power generation, so a possibility exists that a balance between power generation and a decrease in flow velocity will occur at some level. It is necessary to examine how convection behaves with respect to the Lorentz force, which is beyond the scope of this paper.

4.3 Magnetic Diffusivity

In this work, magnetic diffusivity is ignored. The magnetic field should be attenuated depending on the magnetic diffusivity. However, the attenuation term of (13) contains a component corresponding to a magnetic diffusivity of $\frac{1}{\mu\sigma}$ (M_{ij}^{-1} contains $\frac{1}{\mu}$). Therefore, the magnetic diffusivity is already considered in the numerical calculation results. However, the calculation results do not indicate what happens to the magnetic field generated outside the coil. The resistance loss of the fluid outside the convection can be considered as follows.

The loss occurs because of electromagnetic induction due to an increase in current, and the eigenvalue is suppressed. However, this does not mean that the current does not increase. It is a loss caused by an increase in current. That is, the maximum positive eigenvalue is less than that in Table 1 instead of being negative.

4.4 Change in Cross-sectional Area

When a certain amount of fluid moves to the poloidal on convection, the cross-sectional area or flow velocity changes. There is a concern that (13) does not work in these changes. In this paper, the cross-sectional area is set constant, so the flow velocity changes. Then, there is a question whether the derivative of the inductance in the first term on the right side of (13) changes with time with movement, so it cannot be established as an equation. However, since the time derivative is calculated in infinitesimal Δt at the position of the coil set in Fig. 2, it does not change much, so there is no problem with an equation.

4.5 Alternating Matrix Components

The matrix summarizing the right-hand side of (13) contains some alternating matrix components. When calculated, the eigenvalues are real numbers, but they are not the solution of the exact real symmetric matrix. The orthogonality of eigenvectors may be lacking, but at least the calculated eigenvalues are real numbers.

4.6 Relationship with Cowling's Theorem

This argument is contrary to Cowling's theorem. Rather, the argument for Cowling's theorem is incorrect. The fluid is deformed by the poloidal movement of the fluid, and each position of the fluid changes electrically. In addition, electrical mutual influences from each of the other positions are added. Each fluid part is electrically influenced by all other fluid parts. In this work, each of the 16 coils considers the mutual inductance from the other coils. Therefore, it is necessary to solve the electromagnetic induction equations that take into account mutual effects as a simultaneous equation.

Cowling's theorem does not consider this mutual influence. Without considering this mutual influence, the original text of Cowling's theorem argues that the vertex of power generation cannot be maintained. Therefore, a simultaneous equation was not used. This approach is equivalent to ignoring mutual inductance and discussing only self-inductance. A change in self-inductance alone cannot overcome the attenuation even if an electromotive force occurs.

Furthermore, the original text of Cowling's theorem omits important terms for power generation. Since it is a theory of axisymmetry, it is essential to study it strictly in cylindrical coordinates. In cylindrical coordinates, there should be at least one term corresponding to the second term on the right-hand side of (13), but this term is not indicated in the original text of Cowling's theorem.

5 Conclusion

This paper suggests that an axisymmetric magnetic field can be grown from axisymmetric poloidal convection without complex convection. This work also disproves Cowling's theorem.

Declarations

Conflicts of interest

The author has no conflicts of interest to declare.

Funding

No funding was obtained for this work.

Data availability statement

The data described in the manuscript are available. No other data are available.

Clinical trial

not applicable.

Ethics, Consent to Participate, and Consent to Publish declarations

not applicable.

Author contribution statement

Mamoru Otsuki conducted this study and submission independently. He wrote the main manuscript text and prepared all figures. He also programmed the numerical calculation for PC.

Acknowledgements

The study was conducted by only one individual, and there were no direct collaborators. However, we used services such as prepeer review by an editing company, Microsoft's document processing software and its translation function, a multiorder matrix eigenvalue calculation service provided on a website, and draughting software and Adobe Acrobat to draw the diagram. We are grateful for these services and products, which encouraged us to perform this research. We are also grateful for today's inexpensive, high-performance personal computers that can be purchased by individuals and for today's IT world, which offers advanced services.

References

[1] Levy, E.H.: Generation of planetary magnetic fields. Annu. Rev. Earth Planet. Sci. **4**, 159–185 (1976)

[2] Parker, E.N.: Hydromagnetic dynamo models. Astrophysical J. **122**, 293–314 (1955)

[3] Cowling, T.G.: The magnetic field of sunspots. Monthly Notices Roy. Astronomical Soc. **94(1)**, 39–48 (1933)

[4] Masada, Y., Sano, T.: Mean-field modeling of an $\alpha 2$ dynamo coupled with direct numerical simulations of rigidly rotating convection. The Astrophysical Journal Letters **794(1)**, 6 (2014)

[5] Sheremetyeva, Olga V., Godomskaya, Anna N.: The modes of magnetic field generation in a low-mode model of $\alpha\omega$-dynamo with α-generator varying intensity regulated by a function with an alternating kernel. EPJ Web Conf. **254**, 02015 (2021) https://doi.org/10.1051/epjconf/202125402015

[6] M. STEENBECK, F.K., RÄDLER, K.-H.: Berechnung der mittleren lorentz-feldstärke $\overline{b \times B}$ für ein elektrisch leitendes medium in turbulenter, durch coriolis-kräfte beeinflußter bewegung. Institut für Magnetohydrodynamik Jena der Deutschen Akademie der Wissenschaften zu Berlin **21 a**, 369–376 (1966)

[7] J. J. Love, D.G.: Dynamos driven by poloidal flow exist. Geophys. Res. Lett. **23(8)**, 857–860 (1996)

[8] Matthews, P.C.: Dynamo action in simple convective flows. Mathematical, Physical and Engineering Sciences **455**, 1829–1840 (1985)

[9] Cardin, P., Cugliandolo, L.G.: Dynamos: Lecture Notes of the Les Houches Summer School 2007. Les Houches, vol. 88, p. 496. Elsevier Science, Oxford (2011)

[10] Otsuki, M.: Boosting the Magnetic Field of a Toroidal Conductive Fluid by Poloidal Flow. Preprint at https://doi.org/10.51094/jxiv.284 (2023)

[11] Moffatt, K., Dormy, E.: Self-Exciting Fluid Dynamos. Cambridge Texts in Applied Mathematics. Cambridge University Press, Cambridge (2019)

[12] Rojansky, V.B., Rojansky, V.: Electromagnetic Fields and Waves. Dover Books on Physics Series. Dover Publications, New York (1979)